

PAPER • OPEN ACCESS

Search for the doubly heavy baryons Ω_{bc}^0 and Ξ_{bc}^0 decaying to $\Lambda_c^+\pi^-$ and $\Xi_c^+\pi^-$ *

To cite this article: R. Aaij *et al* 2021 *Chinese Phys. C* **45** 093002

View the [article online](#) for updates and enhancements.

You may also like

- [Observation of Gravitational Waves from Two Neutron Star–Black Hole Coalescences](#)
R. Abbott, T. D. Abbott, S. Abraham *et al.*
- [The ATLAS Fast Tracker system](#)
The ATLAS collaboration, G. Aad, B. Abbott *et al.*
- [Diving below the Spin-down Limit: Constraints on Gravitational Waves from the Energetic Young Pulsar PSR J0537-6910](#)
R. Abbott, T. D. Abbott, S. Abraham *et al.*

Search for the doubly heavy baryons Ω_{bc}^0 and Ξ_{bc}^0 decaying to $\Lambda_c^+\pi^-$ and $\Xi_c^+\pi^-$ *

R. Aaij³² C. Abellán Beteta⁵⁰ T. Ackernley⁶⁰ B. Adeva⁴⁶ M. Adinolfi⁵⁴ H. Afsharnia⁹ C.A. Aidala⁸⁵
 S. Aiola²⁵ Z. Ajaltouni⁹ S. Akar⁶⁵ J. Albrecht¹⁵ F. Alessio⁴⁸ M. Alexander⁵⁹ A. Alfonso Alberio⁴⁵
 Z. Aliouche⁶² G. Alkhazov³⁸ P. Alvarez Cartelle⁵⁵ S. Amato² Y. Amhis¹¹ L. An⁴⁸ L. Anderlini²²
 A. Andreianov³⁸ M. Andreotti²¹ F. Archilli¹⁷ A. Artamonov⁴⁴ M. Artuso⁶⁸ K. Arzymatov⁴² E. Aslanides¹⁰
 M. Atzeni⁵⁰ B. Audurier¹² S. Bachmann¹⁷ M. Bachmayer⁴⁹ J.J. Back⁵⁶ P. Baladron Rodriguez⁴⁶ V. Balagura¹²
 W. Baldini²¹ J. Baptista Leite¹ R.J. Barlow⁶² S. Barsuk¹¹ W. Barter⁶¹ M. Bartolini²⁴ F. Baryshnikov⁸²
 J.M. Basels¹⁴ G. Bassi²⁹ B. Batsukh⁶⁸ A. Battig¹⁵ A. Bay⁴⁹ M. Becker¹⁵ F. Bedeschi²⁹ I. Bediaga¹
 A. Beiter⁶⁸ V. Belavin⁴² S. Belin²⁷ V. Bellee⁴⁹ K. Belous⁴⁴ I. Belov⁴⁰ I. Belyaev⁴¹ G. Bencivenni²³
 E. Ben-Haim¹³ A. Berezhnoy⁴⁰ R. Bernet⁵⁰ D. Berninghoff¹⁷ H.C. Bernstein⁶⁸ C. Bertella⁴⁸ A. Bertolin⁸²
 C. Betancourt⁵⁰ F. Betti⁴⁸ Ia. Bezshyiko⁵⁰ S. Bhasin⁵⁴ J. Bhom³⁵ L. Bian⁷³ M.S. Bieker¹⁵ S. Bifani⁵³
 P. Billoir¹³ M. Birch⁶¹ F.C.R. Bishop⁵⁵ A. Bitadze⁶² A. Bizzeti^{22,k} M. Bjørn⁶³ M.P. Blago⁴⁸ T. Blake⁵⁶
 F. Blanc⁴⁹ S. Blusk⁶⁸ D. Bobulska⁵⁹ J.A. Boelhauve¹⁵ O. Boente Garcia⁴⁶ T. Boettcher⁶⁴ A. Boldyrev⁸¹
 A. Bondar⁴³ N. Bondar^{38,48} S. Borghi⁶² M. Borisyak⁴² M. Borsato¹⁷ J.T. Borsuk³⁵ S.A. Bouchiba⁴⁹
 T.J.V. Bowcock⁶⁰ A. Boyer⁴⁸ C. Bozzi²¹ M.J. Bradley⁶¹ S. Braun⁶⁶ A. Brea Rodriguez⁴⁶ M. Brodski⁴⁸
 J. Brodzicka³⁵ A. Brossa Gonzalo⁵⁶ D. Brundu²⁷ A. Buonauro⁵⁰ C. Burr⁴⁸ A. Bursche⁷² A. Butkevich³⁹
 J.S. Butter³² J. Buytaert⁴⁸ W. Byczynski⁴⁸ S. Cadeddu²⁷ H. Cai⁷³ R. Calabrese^{21,f} L. Calefice^{15,13}
 L. Calero Diaz²³ S. Cali²³ R. Calladine⁵³ M. Calvi^{26,j} M. Calvo Gomez⁸⁴ P. Camargo Magalhaes⁵⁴
 A. Camboni^{45,84} P. Campana²³ A.F. Campoverde Quezada⁶ S. Capelli^{26,j} L. Capriotti^{20,d} A. Carbone^{20,d}
 G. Carboni³¹ R. Cardinale²⁴ A. Cardini²⁷ I. Carli⁴ P. Carniti^{26,j} L. Carus¹⁴ K. Carvalho Akiba³²
 A. Casais Vidal⁴⁶ G. Casse⁶⁰ M. Cattaneo⁴⁸ G. Cavallero⁴⁸ S. Celani⁴⁹ J. Cerasoli¹⁰ A.J. Chadwick⁶⁰
 M.G. Chapman⁵⁴ M. Charles¹³ Ph. Charpentier⁴⁸ G. Chatzikonstantinidis⁵³ C.A. Chavez Barajas⁶⁰
 M. Chefdeville⁸ C. Chen³ S. Chen⁴ A. Chernov³⁵ V. Chobanova⁴⁶ S. Cholak⁴⁹ M. Chrzaszcz³⁵
 A. Chubykin³⁸ V. Chulikov³⁸ P. Ciambriano²³ M.F. Cicala⁵⁶ X. Cid Vidal⁴⁶ G. Ciezarek⁴⁸ P.E.L. Clarke⁵⁸
 M. Clemencic⁴⁸ H.V. Cliff⁵⁵ J. Closier⁴⁸ J.L. Cobbedick⁶² V. Coco⁴⁸ J.A.B. Coelho¹¹ J. Cogan¹⁰
 E. Cogneras⁹ L. Cojocariu³⁷ P. Collins⁴⁸ T. Colombo⁴⁸ L. Congedo^{19,c} A. Contu²⁷ N. Cooke⁵³ G. Coombs⁵⁹
 G. Corti⁴⁸ C.M. Costa Sobral⁵⁶ B. Couturier⁴⁸ D.C. Craik⁶⁴ J. Crkovská⁶⁷ M. Cruz Torres¹ R. Currie⁵⁸
 C.L. Da Silva⁶⁷ E. Dall'Occo¹⁵ J. Dalseno⁴⁶ C. D'Ambrosio⁴⁸ A. Danilina⁴¹ P. d'Argent⁴⁸ A. Davis⁶²
 O. De Aguiar Francisco⁶² K. De Bruyn⁷⁸ S. De Capua⁶² M. De Cian⁴⁹ J.M. De Miranda¹ L. De Paula²
 M. De Serio^{19,c} D. De Simone⁵⁰ P. De Simone²³ J.A. de Vries⁷⁹ C.T. Dean⁶⁷ D. Decamp⁸ L. Del Buono¹³
 B. Delaney⁵⁵ H.-P. Dembinski¹⁵ A. Dendek³⁴ V. Denysenko⁵⁰ D. Derkach⁸¹ O. Deschamps⁹ F. Desse¹¹
 F. Dettori^{27,e} B. Dey⁷³ P. Di Nezza²³ S. Didenko⁸² L. Dieste Maronas⁴⁶ H. Dijkstra⁴⁸ V. Dobishuk⁵²

Received 27 May 2021; Accepted 18 June 2021; Published online 16 August 2021

* We acknowledge support from CERN and from the national agencies: CAPES, CNPq, FAPERJ and FINEP (Brazil); MOST and NSFC (China); CNRS/IN2P3 (France); BMBF, DFG and MPG (Germany); INFN (Italy); NWO (Netherlands); MNiSW and NCN (Poland); MEN/IFA (Romania); MSHE (Russia); MICINN (Spain); SNSF and SER (Switzerland); NASU (Ukraine); STFC (United Kingdom); DOE NP and NSF (USA). We acknowledge the computing resources that are provided by CERN, IN2P3 (France), KIT and DESY (Germany), INFN (Italy), SURF (Netherlands), PIC (Spain), GridPP (United Kingdom), RRCKI and Yandex LLC (Russia), CSCS (Switzerland), IFIN-HH (Romania), CBPF (Brazil), PL-GRID (Poland) and NERSC (USA). We are indebted to the communities behind the multiple open-source software packages on which we depend. Individual groups or members have received support from ARC and ARDC (Australia); AvH Foundation (Germany); EPLAN-ET, Marie Skłodowska-Curie Actions and ERC (European Union); A*MIDEX, ANR, Labex P2IO and OCEVU, and Région Auvergne-Rhône-Alpes (France); Key Research Program of Frontier Sciences of CAS, CAS PIFI, CAS CCEPP, Fundamental Research Funds for the Central Universities, and Sci. Tech. Program of Guangzhou (China); RFBR, RSF and Yandex LLC (Russia); GVA, XuntaGal and GENCAT (Spain); the Leverhulme Trust, the Royal Society and UKRI (United Kingdom)

† E-mail: shiyang.li@cern.ch



Content from this work may be used under the terms of the Creative Commons Attribution 3.0 licence. Any further distribution of this work must maintain attribution to the author(s) and the title of the work, journal citation and DOI. Article funded by SCOAP³ and published under licence by Chinese Physical Society and the Institute of High Energy Physics of the Chinese Academy of Sciences and the Institute of Modern Physics of the Chinese Academy of Sciences and IOP Publishing Ltd

A.M. Donohoe¹⁸ F. Dordei²⁷ A.C. dos Reis¹ L. Douglas⁵⁹ A. Dovbnya⁵¹ A.G. Downes⁸ K. Dreimanis⁶⁰
 M.W. Dudek³⁵ L. Dufour⁴⁸ V. Duk⁷⁷ P. Durante⁴⁸ J.M. Durham⁶⁷ D. Dutta⁶² A. Dziurda³⁵ A. Dzyuba³⁸
 S. Easo⁵⁷ U. Egede⁶⁹ V. Egorychev⁴¹ S. Eidelman^{43,v} S. Eisenhardt⁵⁸ S. Ek-In⁴⁹ L. Eklund^{59,w} S. Ely⁶⁸
 A. Ene³⁷ E. Epple⁶⁷ S. Escher¹⁴ J. Eschle⁵⁰ S. Esen¹³ T. Evans⁴⁸ A. Falabella²⁰ J. Fan³ Y. Fan⁶ B. Fang⁷³
 S. Farry⁶⁰ D. Fazzini^{26,j} M. Féo⁴⁸ A. Fernandez Prieto⁴⁶ J.M. Fernandez-tenllado Arribas⁴⁵ F. Ferrari^{20,d}
 L. Ferreira Lopes⁴⁹ F. Ferreira Rodrigues² S. Ferreres Sole³² M. Ferrillo⁵⁰ M. Ferro-Luzzi⁴⁸ S. Filippov³⁹
 R.A. Fini¹⁹ M. Fiorini^{21,f} M. Firlje³⁴ K.M. Fischer⁶³ C. Fitzpatrick⁶² T. Fiutowski³⁴ F. Fleuret¹² M. Fontana¹³
 F. Fontanelli^{24,h} R. Forty⁴⁸ V. Franco Lima⁶⁰ M. Franco Sevilla⁶⁶ M. Frank⁴⁸ E. Franzoso²¹ G. Frau¹⁷
 C. Frei⁴⁸ D.A. Friday⁵⁹ J. Fu²⁵ Q. Fuehring¹⁵ W. Funk⁴⁸ E. Gabriel³² T. Gaintseva⁴² A. Gallas Torreira⁴⁶
 D. Galli^{20,d} S. Gambetta^{58,48} Y. Gan³ M. Gandelman² P. Gandini²⁵ Y. Gao⁵ M. Garau²⁷ L.M. Garcia Martin⁵⁶
 P. Garcia Moreno⁴⁵ J. García Pardiñas^{26,j} B. Garcia Plana⁴⁶ F.A. Garcia Rosales¹² L. Garrido⁴⁵ C. Gaspar⁴⁸
 R.E. Geertsema³² D. Gerick¹⁷ L.L. Gerken¹⁵ E. Gersabeck⁶² M. Gersabeck⁶² T. Gershon⁵⁶ D. Gerstel¹⁰
 Ph. Ghez⁸ V. Gibson⁵⁵ H.K. Gienza³⁶ M. Giovannetti^{23,p} A. Gioventù⁴⁶ P. Gironella Gironell⁴⁵ L. Giubega³⁷
 C. Giugliano^{21,f,48} K. Gizdov⁵⁸ E.L. Gkougkousis⁴⁸ V.V. Gligorov¹³ C. Göbel⁷⁰ E. Golobardes⁸⁴ D. Golubkov⁴¹
 A. Golutvin^{61,82} A. Gomes^{1,a} S. Gomez Fernandez⁴⁵ F. Goncalves Abrantes⁶³ M. Goncerz³⁵ G. Gong³
 P. Gorbounov⁴¹ I.V. Gorelov⁴⁰ C. Gotti²⁶ E. Govorkova⁴⁸ J.P. Grabowski¹⁷ T. Grammatico¹³
 L.A. Granado Cardoso⁴⁸ E. Graugés⁴⁵ E. Graverini⁴⁹ G. Graziani²² A. Grecu³⁷ L.M. Greeven³² P. Griffith^{21,f}
 L. Grillo⁶² S. Gromov⁸² B.R. Gruberg Cazon⁶³ C. Gu³ M. Guarise²¹ P. A. Günther¹⁷ E. Gushchin³⁹ A. Guth¹⁴
 Y. Guz^{44,48} T. Gys⁴⁸ T. Hadavizadeh⁶⁹ G. Haefeli⁴⁹ C. Haen⁴⁸ J. Haimberger⁴⁸ T. Halewood-leagas⁶⁰
 P.M. Hamilton⁶⁶ Q. Han⁷ X. Han¹⁷ T.H. Hancock⁶³ S. Hansmann-Menzemer¹⁷ N. Harnew⁶³ T. Harrison⁶⁰
 C. Hasse⁴⁸ M. Hatch⁴⁸ J. He^{6,b} M. Hecker⁶¹ K. Heijhoff³² K. Heinicke¹⁵ A.M. Hennequin⁴⁸ K. Hennessy⁶⁰
 L. Henry^{25,47} J. Heuel¹⁴ A. Hicheur² D. Hill⁴⁹ M. Hilton⁶² S.E. Hollitt¹⁵ J. Hu¹⁷ J. Hu⁷² W. Hu⁷
 W. Huang⁶ X. Huang⁷³ W. Hulsbergen³² R.J. Hunter⁵⁶ M. Hushchyn⁸¹ D. Hutchcroft⁶⁰ D. Hynds³² P. Ibis¹⁵
 M. Idzik³⁴ D. Ilin³⁸ P. Ilten⁶⁵ A. Inglessi³⁸ A. Ishteev⁸² K. Ivshin³⁸ R. Jacobsson⁴⁸ S. Jakobsen⁴⁸ E. Jans³²
 B.K. Jashai⁴⁷ A. Jawahery⁶⁶ V. Jevtic¹⁵ M. Jezabek³⁵ F. Jiang³ M. John⁶³ D. Johnson⁴⁸ C.R. Jones⁵⁵
 T.P. Jones⁵⁶ B. Jost⁴⁸ N. Jurik⁴⁸ S. Kandybei⁵¹ Y. Kang³ M. Karacson⁴⁸ M. Karpov⁸¹ F. Keizer⁴⁸
 M. Kenzie⁵⁶ T. Ketel³³ B. Khanji¹⁵ A. Kharisova⁸³ S. Kholodenko⁴⁴ T. Kirn¹⁴ V.S. Kirsebom⁴⁹ O. Kitouni⁶⁴
 S. Klaver³² K. Klimaszewski³⁶ S. Koliiev⁵² A. Kondybayeva⁸² A. Konoplyannikov⁴¹ P. Kopciwicz³⁴
 R. Kopečna¹⁷ P. Koppenburg³² M. Korolev⁴⁰ I. Kostiuk^{32,52} O. Kot⁵² S. Kotriakhova^{21,38} P. Kravchenko³⁸
 L. Kravchuk³⁹ R.D. Krawczyk⁴⁸ M. Krepš⁵⁶ F. Kress⁶¹ S. Kretzschmar¹⁴ P. Krokovny^{43,v} W. Krupa³⁴
 W. Krzemien³⁶ W. Kucewicz^{35,t} M. Kucharczyk³⁵ V. Kudryavtsev^{43,v} H.S. Kuindersma³² G.J. Kunde⁶⁷
 T. Kvaratskheliya⁴¹ D. Lacarrere⁴⁸ G. Lafferty⁶² A. Lai²⁷ A. Lampis²⁷ D. Lancierini⁵⁰ J.J. Lane⁶² R. Lane⁵⁴
 G. Lanfranchi²³ C. Langenbruch¹⁴ J. Langer¹⁵ O. Lantwin⁵⁰ T. Latham⁵⁶ F. Lazzari^{29,q} R. Le Gac¹⁰
 S.H. Lee⁸⁵ R. Lefèvre⁹ A. Leflat⁴⁰ S. Legotin⁸² O. Leroy¹⁰ T. Lesiak³⁵ B. Leverington¹⁷ H. Li⁷² L. Li⁶³
 P. Li¹⁷ S. Li⁷⁴ Y. Li⁴ Y. Li⁴ Z. Li⁶⁸ X. Liang⁶⁸ T. Lin⁶¹ R. Lindner⁴⁸ V. Lisovskyi¹⁵ R. Litvinov²⁷
 G. Liu⁷² H. Liu⁶ S. Liu⁴ X. Liu³ A. Loi²⁷ J. Lomba Castro⁴⁶ I. Longstaff⁵⁹ J.H. Lopes² G.H. Lovell⁵⁵
 Y. Lu⁴ D. Lucchesi^{28,1} S. Luchuk³⁹ M. Lucio Martinez³² V. Lukashenko³² Y. Luo³ A. Lupato⁶² E. Luppi^{21,f}
 O. Lupton⁵⁶ A. Lusiani^{29,m} X. Lyu⁶ L. Ma⁴ R. Ma⁶ S. Maccolini^{20,d} F. Machefer¹¹ F. Maciuc³⁷
 V. Macko⁴⁹ P. Mackowiak¹⁵ S. Maddrell-Mander⁵⁴ O. Madejczyk³⁴ L.R. Madhan Mohan⁵⁴ O. Maev³⁸
 A. Maevskiy⁸¹ D. Maisuzenko³⁸ M.W. Majewski³⁴ J.J. Malczewski³⁵ S. Malde⁶³ B. Malecki⁴⁸ A. Malinin⁸⁰
 T. Maltsev^{43,v} H. Malygina¹⁷ G. Manca^{27,e} G. Mancinelli¹⁰ D. Manuzzi^{20,d} D. Marangotto^{25,i} J. Maratas^{9,s}
 J.F. Marchand⁸ U. Marconi²⁰ S. Mariani^{22,g} C. Marin Benito¹¹ M. Marinangeli⁴⁹ P. Marino^{49,m} J. Marks¹⁷
 A.M. Marshall⁵⁴ P.J. Marshall⁶⁰ G. Martellotti³⁰ L. Martinazzoli^{48,j} M. Martinelli^{26,j} D. Martinez Santos⁴⁶
 F. Martinez Vidal⁴⁷ A. Massafferri¹ M. Materok¹⁴ R. Matev⁴⁸ A. Mathad⁵⁰ Z. Mathe⁴⁸ V. Matiunin⁴¹
 C. Matteuzzi²⁶ K.R. Mattioli⁸⁵ A. Mauri³² E. Maurice¹² J. Mauricio⁴⁵ M. Mazurek⁴⁸ M. McCann⁶¹
 L. McConnell¹⁸ T.H. Mcgrath⁶² A. McNab⁶² R. McNulty¹⁸ J.V. Mead⁶⁰ B. Meadows⁶⁵ C. Meaux¹⁰

G. Meier¹⁵ N. Meinert⁷⁶ D. Melnychuk³⁶ S. Meloni^{26,j} M. Merk^{32,79} A. Merli²⁵ L. Meyer Garcia²
M. Mikhasenko⁴⁸ D.A. Milanes⁷⁴ E. Millard⁵⁶ M. Milovanovic⁴⁸ M.-N. Minard⁸ A. Minotti²¹ L. Minzoni^{21,f}
S.E. Mitchell⁵⁸ B. Mitreska⁶² D.S. Mitzel⁴⁸ A. Mödden¹⁵ R.A. Mohammed⁶³ R.D. Moise⁶¹ T. Mombächer¹⁵
I.A. Monroy⁷⁴ S. Monteil⁹ M. Morandin²⁸ G. Morello²³ M.J. Morello^{29,m} J. Moron³⁴ A.B. Morris⁷⁵
A.G. Morris⁵⁶ R. Mountain⁶⁸ H. Mu³ F. Muheim^{58,48} M. Mukherjee⁷ M. Mulder⁴⁸ D. Müller⁴⁸ K. Müller⁵⁰
C.H. Murphy⁶³ D. Murray⁶² P. Muzzetto^{27,48} P. Naik⁵⁴ T. Nakada⁴⁹ R. Nandakumar⁵⁷ T. Nanut⁴⁹ I. Nasteva²
M. Needham⁵⁸ I. Neri²¹ N. Neri^{25,i} S. Neubert⁷⁵ N. Neufeld⁴⁸ R. Newcombe⁶¹ T.D. Nguyen⁴⁹
C. Nguyen-Mau^{49,x} E.M. Niel¹¹ S. Nieswand¹⁴ N. Nikitin⁴⁰ N.S. Nolte⁴⁸ C. Nunez⁸⁵ A. Oblakowska-Mucha³⁴
V. Obraztsov⁴⁴ D.P. O'Hanlon⁵⁴ R. Oldeman^{27,e} M.E. Olivares⁶⁸ C.J.G. Onderwater⁷⁸ A. Ossowska³⁵
J.M. Otorola Goicochea² T. Ovsianikova⁴¹ P. Owen⁵⁰ A. Oyanguren⁴⁷ B. Pagare⁵⁶ P.R. Pais⁴⁸ T. Pajero⁶³
A. Palano¹⁹ M. Palutan²³ Y. Pan⁶² G. Panshin⁸³ A. Papanestis⁵⁷ M. Pappagallo^{19,c} L.L. Pappalardo^{21,f}
C. Pappenheimer⁶⁵ W. Parker⁶⁶ C. Parkes⁶² C.J. Parkinson⁴⁶ B. Passalacqua²¹ G. Passaleva²² A. Pastore¹⁹
M. Patel⁶¹ C. Patrignani^{20,d} C.J. Pawley⁷⁹ A. Pearce⁴⁸ A. Pellegrino³² M. Pepe Altarelli⁴⁸ S. Perazzini²⁰
D. Pereima⁴¹ P. Perret⁹ M. Petric^{59,48} K. Petridis⁵⁴ A. Petrolini^{24,h} A. Petrov⁸⁰ S. Petrucci⁵⁸ M. Petruzzo²⁵
T.T.H. Pham⁶⁸ A. Philippov⁴² L. Pica^{29,n} M. Piccini⁷⁷ B. Pietrzyk⁸ G. Pietrzyk⁴⁹ M. Pili⁶³ D. Pinci³⁰
F. Pisani⁴⁸ P.K. Resmi¹⁰ V. Placinta³⁷ J. Plews⁵³ M. Plo Casasus⁴⁶ F. Polci¹³ M. Poli Lener²³ M. Poliakov⁶⁸
A. Poluektov¹⁰ N. Polukhina^{82,u} I. Polyakov⁶⁸ E. Polycarpo² G.J. Pomery⁵⁴ S. Ponce⁴⁸ D. Popov^{6,48}
S. Popov⁴² S. Poslavskii⁴⁴ K. Prasanth³⁵ L. Promberger⁴⁸ C. Prouve⁴⁶ V. Pugatch⁵² H. Pullen⁶³ G. Punzi^{29,n}
W. Qian⁶ J. Qin⁶ R. Quagliani¹³ B. Quintana⁸ N.V. Raab¹⁸ R.I. Rabadan Trejo¹⁰ B. Rachwal³⁴
J.H. Rademacker⁵⁴ M. Rama²⁹ M. Ramos Pernas⁵⁶ M.S. Rangel² F. Ratnikov^{42,81} G. Raven³³ M. Reboud⁸
F. Redi⁴⁹ F. Reiss⁶² C. Remon Alepuz⁴⁷ Z. Ren³ V. Renaudin⁶³ R. Ribatti²⁹ S. Ricciardi⁵⁷ K. Rinnert⁶⁰
P. Robbe¹¹ A. Robert¹³ G. Robertson⁵⁸ A.B. Rodrigues⁴⁹ E. Rodrigues⁶⁰ J.A. Rodriguez Lopez⁷⁴ A. Rollings⁶³
P. Roloff⁴⁸ V. Romanovskiy⁴⁴ M. Romero Lamas⁴⁶ A. Romero Vidal⁴⁶ J.D. Roth⁸⁵ M. Rotondo²³
M.S. Rudolph⁶⁸ T. Rui⁴⁸ J. Ruiz Vidal⁴⁷ A. Ryzhikov⁸¹ J. Ryzka³⁴ J.J. Saborido Silva⁴⁶ N. Sagidova³⁸
N. Sahoo⁵⁶ B. Saitta^{27,e} D. Sanchez Gonzalo⁴⁵ C. Sanchez Gras³² R. Santacesaria³⁰ C. Santamarina Rios⁴⁶
M. Santimaria²³ E. Santovetti^{31,p} D. Saranin⁸² G. Sarpis⁵⁹ M. Sarpis⁷⁵ A. Sarti³⁰ C. Satriano^{30,o} A. Satta³¹
M. Saur¹⁵ D. Savrina^{41,40} H. Sazak⁹ L.G. Scantlebury Smead⁶³ S. Schael¹⁴ M. Schellenberg¹⁵ M. Schiller⁵⁹
H. Schindler⁴⁸ M. Schmelling¹⁶ B. Schmidt⁴⁸ O. Schneider⁴⁹ A. Schopper⁴⁸ M. Schubiger³² S. Schulte⁴⁹
M.H. Schune¹¹ R. Schwemmer⁴⁸ B. Sciascia²³ S. Sellam⁴⁶ A. Semennikov⁴¹ M. Senghi Soares³³ A. Sergi^{24,48}
N. Serra⁵⁰ L. Sestini²⁸ A. Seuthe¹⁵ P. Seyfert⁴⁸ Y. Shang⁵ D.M. Shangase⁸⁵ M. Shapkin⁴⁴ I. Shchemerov⁸²
L. Shchutska⁴⁹ T. Shears⁶⁰ L. Shekhtman^{43,v} Z. Shen⁵ V. Shevchenko⁸⁰ E.B. Shields^{26,j} E. Shmanin⁸²
J.D. Shupperd⁶⁸ B.G. Siddi²¹ R. Silva Coutinho⁵⁰ G. Simi²⁸ S. Simone^{19,c} N. Skidmore⁶² T. Skwarnicki⁶⁸
M.W. Slater⁵³ I. Slazyk^{21,f} J.C. Smallwood⁶³ J.G. Smeaton⁵⁵ A. Smetkina⁴¹ E. Smith¹⁴ M. Smith⁶¹
A. Snoch³² M. Soares²⁰ L. Soares Lavoura⁹ M.D. Sokoloff⁶⁵ F.J.P. Soler⁵⁹ A. Solovov³⁸ I. Solov'yev³⁸
F.L. Souza De Almeida² B. Souza De Paula² B. Spaan¹⁵ E. Spadaro Norella^{25,i} P. Spradlin⁵⁹ F. Stagni⁴⁸
M. Stahl⁶⁵ S. Stahl⁴⁸ P. Stefko⁴⁹ O. Steinkamp^{50,82} O. Stenyakin⁴⁴ H. Stevens¹⁵ S. Stone⁶⁸ M.E. Stramaglia⁴⁹
M. Straticiu³⁷ D. Strelakina⁸² F. Suljik⁶³ J. Sun²⁷ L. Sun⁷³ Y. Sun⁶⁶ P. Svihra⁶² P.N. Swallow⁵³
K. Swientek³⁴ A. Szabelski³⁶ T. Szumlak³⁴ M. Szymanski⁴⁸ S. Taneja⁶² F. Teubert⁴⁸ E. Thomas⁴⁸
K.A. Thomson⁶⁰ V. Tisserand⁹ S. T'Jampens⁸ M. Tobin⁴ L. Tomassetti^{21,f} D. Torres Machado¹ D.Y. Tou¹³
M.T. Tran⁴⁹ E. Trifonova⁸² C. Trippl⁴⁹ G. Tuci^{29,n} A. Tully⁴⁹ N. Tuning^{32,48} A. Ukleja³⁶ D.J. Unverzagt¹⁷
E. Ursov⁸² A. Usachov³² A. Ustyuzhanin^{42,81} U. Uwer¹⁷ A. Vagner⁸³ V. Vagnoni²⁰ A. Valassi⁴⁸ G. Valenti²⁰
N. Valls Canudas⁸⁴ M. van Beuzekom³² M. Van Dijk⁴⁹ E. van Herwijnen⁸² C.B. Van Hulse¹⁸ M. van Veghel⁷⁸
R. Vazquez Gomez⁴⁶ P. Vazquez Regueiro⁴⁶ C. Vázquez Sierra⁴⁸ S. Vecchi²¹ J.J. Velthuis⁵⁴ M. Veltri^{22,r}
A. Venkateswaran⁶⁸ M. Veronesi³² M. Vesterinen⁵⁶ D. Vieira⁶⁵ M. Vieites Diaz⁴⁹ H. Viemann⁷⁶
X. Vilasis-Cardona⁸⁴ E. Vilella Figueras⁶⁰ P. Vincent¹³ G. Vitali²⁹ D. Vom Bruch¹⁰ A. Vorobyev³⁸
V. Vorobyev^{43,v} N. Voropaev³⁸ R. Waldi⁷⁶ J. Walsh²⁹ C. Wang¹⁷ J. Wang⁵ J. Wang⁴ J. Wang³ J. Wang⁷³

M. Wang³ R. Wang⁵⁴ Y. Wang⁷ Z. Wang⁵⁰ Z. Wang³ H.M. Wark⁶⁰ N.K. Watson⁵³ S.G. Weber¹³
 D. Websdale⁶¹ C. Weisser⁶⁴ B.D.C. Westhenry⁵⁴ D.J. White⁶² M. Whitehead⁵⁴ D. Wiedner¹⁵ G. Wilkinson⁶³
 M. Wilkinson⁶⁸ I. Williams⁵⁵ M. Williams⁶⁴ M.R.J. Williams⁵⁸ F.F. Wilson⁵⁷ W. Wislicki³⁶ M. Witek³⁵
 L. Witola¹⁷ G. Wormser¹¹ S.A. Wotton⁵⁵ H. Wu⁶⁸ K. Wyllie⁴⁸ Z. Xiang⁶ D. Xiao⁷ Y. Xie⁷ A. Xu⁵
 J. Xu⁶ L. Xu³ M. Xu⁷ Q. Xu⁶ Z. Xu⁵ Z. Xu⁶ D. Yang³ S. Yang⁶ Y. Yang⁶ Z. Yang³ Z. Yang⁶⁶
 Y. Yao⁶⁸ L.E. Yeomans⁶⁰ H. Yin⁷ J. Yu⁷¹ X. Yuan⁶⁸ O. Yushchenko⁴⁴ E. Zaffaroni⁴⁹ M. Zavertyaev^{16,u}
 M. Zdybal³⁵ O. Zenaiev⁴⁸ M. Zeng³ D. Zhang⁷ L. Zhang³ S. Zhang⁵ Y. Zhang⁵ Y. Zhang⁶³ A. Zhelezov¹⁷
 Y. Zheng⁶ X. Zhou⁶ Y. Zhou⁶ X. Zhu³ V. Zhukov^{14,40} J.B. Zonneveld⁵⁸ Q. Zou⁴ S. Zucchelli^{20,d}
 D. Zuliani²⁸ G. Zunica⁶²
 (LHCb Collaboration)

¹Centro Brasileiro de Pesquisas Físicas (CBPF), Rio de Janeiro, Brazil

²Universidade Federal do Rio de Janeiro (UFRJ), Rio de Janeiro, Brazil

³Center for High Energy Physics, Tsinghua University, Beijing, China

⁴Institute Of High Energy Physics (IHEP), Beijing, China

⁵School of Physics State Key Laboratory of Nuclear Physics and Technology, Peking University, Beijing, China

⁶University of Chinese Academy of Sciences, Beijing, China

⁷Institute of Particle Physics, Central China Normal University, Wuhan, Hubei, China

⁸Univ. Savoie Mont Blanc, CNRS, IN2P3-LAPP, Annecy, France

⁹Université Clermont Auvergne, CNRS/IN2P3, LPC, Clermont-Ferrand, France

¹⁰Aix Marseille Univ, CNRS/IN2P3, CPPM, Marseille, France

¹¹Université Paris-Saclay, CNRS/IN2P3, IJCLab, Orsay, France

¹²Laboratoire Leprince-Ringuet, CNRS/IN2P3, Ecole Polytechnique, Institut Polytechnique de Paris, Palaiseau, France

¹³LPNHE, Sorbonne Université, Paris Diderot Sorbonne Paris Cité, CNRS/IN2P3, Paris, France

¹⁴I. Physikalisches Institut, RWTH Aachen University, Aachen, Germany

¹⁵Fakultät Physik, Technische Universität Dortmund, Dortmund, Germany

¹⁶Max-Planck-Institut für Kernphysik (MPIK), Heidelberg, Germany

¹⁷Physikalisches Institut, Ruprecht-Karls-Universität Heidelberg, Heidelberg, Germany

¹⁸School of Physics, University College Dublin, Dublin, Ireland

¹⁹INFN Sezione di Bari, Bari, Italy

²⁰INFN Sezione di Bologna, Bologna, Italy

²¹INFN Sezione di Ferrara, Ferrara, Italy

²²INFN Sezione di Firenze, Firenze, Italy

²³INFN Laboratori Nazionali di Frascati, Frascati, Italy

²⁴INFN Sezione di Genova, Genova, Italy

²⁵INFN Sezione di Milano, Milano, Italy

²⁶INFN Sezione di Milano-Bicocca, Milano, Italy

²⁷INFN Sezione di Cagliari, Monserrato, Italy

²⁸Università degli Studi di Padova, Università e INFN, Padova, Padova, Italy

²⁹INFN Sezione di Pisa, Pisa, Italy

³⁰INFN Sezione di Roma La Sapienza, Roma, Italy

³¹INFN Sezione di Roma Tor Vergata, Roma, Italy

³²Nikhef National Institute for Subatomic Physics, Amsterdam, Netherlands

³³Nikhef National Institute for Subatomic Physics and VU University Amsterdam, Amsterdam, Netherlands

³⁴AGH - University of Science and Technology, Faculty of Physics and Applied Computer Science, Kraków, Poland

³⁵Henryk Niewodniczanski Institute of Nuclear Physics Polish Academy of Sciences, Kraków, Poland

³⁶National Center for Nuclear Research (NCBJ), Warsaw, Poland

³⁷Horia Hulubei National Institute of Physics and Nuclear Engineering, Bucharest-Magurele, Romania

³⁸Petersburg Nuclear Physics Institute NRC Kurchatov Institute (PNPI NRC KI), Gatchina, Russia

³⁹Institute for Nuclear Research of the Russian Academy of Sciences (INR RAS), Moscow, Russia

⁴⁰Institute of Nuclear Physics, Moscow State University (SINP MSU), Moscow, Russia

⁴¹Institute of Theoretical and Experimental Physics NRC Kurchatov Institute (ITEP NRC KI), Moscow, Russia

⁴²Yandex School of Data Analysis, Moscow, Russia

⁴³Budker Institute of Nuclear Physics (SB RAS), Novosibirsk, Russia

⁴⁴Institute for High Energy Physics NRC Kurchatov Institute (IHEP NRC KI), Protvino, Russia, Protvino, Russia

⁴⁵ICCUB, Universitat de Barcelona, Barcelona, Spain

⁴⁶Instituto Galego de Física de Altas Enerxías (IGFAE), Universidade de Santiago de Compostela, Santiago de Compostela, Spain

⁴⁷Instituto de Física Corpuscular, Centro Mixto Universidad de Valencia - CSIC, Valencia, Spain

⁴⁸European Organization for Nuclear Research (CERN), Geneva, Switzerland

⁴⁹Institute of Physics, Ecole Polytechnique Fédérale de Lausanne (EPFL), Lausanne, Switzerland

⁵⁰Physik-Institut, Universität Zürich, Zürich, Switzerland

⁵¹NSC Kharkiv Institute of Physics and Technology (NSC KIPT), Kharkiv, Ukraine

⁵²Institute for Nuclear Research of the National Academy of Sciences (KINR), Kyiv, Ukraine

⁵³University of Birmingham, Birmingham, United Kingdom

- ⁵⁴H.H. Wills Physics Laboratory, University of Bristol, Bristol, United Kingdom
⁵⁵Cavendish Laboratory, University of Cambridge, Cambridge, United Kingdom
⁵⁶Department of Physics, University of Warwick, Coventry, United Kingdom
⁵⁷STFC Rutherford Appleton Laboratory, Didcot, United Kingdom
⁵⁸School of Physics and Astronomy, University of Edinburgh, Edinburgh, United Kingdom
⁵⁹School of Physics and Astronomy, University of Glasgow, Glasgow, United Kingdom
⁶⁰Oliver Lodge Laboratory, University of Liverpool, Liverpool, United Kingdom
⁶¹Imperial College London, London, United Kingdom
⁶²Department of Physics and Astronomy, University of Manchester, Manchester, United Kingdom
⁶³Department of Physics, University of Oxford, Oxford, United Kingdom
⁶⁴Massachusetts Institute of Technology, Cambridge, MA, United States
⁶⁵University of Cincinnati, Cincinnati, OH, United States
⁶⁶University of Maryland, College Park, MD, United States
⁶⁷Los Alamos National Laboratory (LANL), Los Alamos, United States
⁶⁸Syracuse University, Syracuse, NY, United States
⁶⁹School of Physics and Astronomy, Monash University, Melbourne, Australia, associated to ⁵⁶
⁷⁰Pontificia Universidade Católica do Rio de Janeiro (PUC-Rio), Rio de Janeiro, Brazil, associated to ²
⁷¹Physics and Micro Electronic College, Hunan University, Changsha City, China, associated to ⁷
⁷²Guangdong Provincial Key Laboratory of Nuclear Science, Institute of Quantum Matter, South China Normal University, Guangzhou, China, associated to ³
⁷³School of Physics and Technology, Wuhan University, Wuhan, China, associated to ³
⁷⁴Departamento de Física, Universidad Nacional de Colombia, Bogota, Colombia, associated to ¹³
⁷⁵Universität Bonn - Helmholtz-Institut für Strahlen und Kernphysik, Bonn, Germany, associated to ¹⁷
⁷⁶Institut für Physik, Universität Rostock, Rostock, Germany, associated to ¹⁷
⁷⁷INFN Sezione di Perugia, Perugia, Italy, associated to ²¹
⁷⁸Van Swinderen Institute, University of Groningen, Groningen, Netherlands, associated to ³²
⁷⁹Universiteit Maastricht, Maastricht, Netherlands, associated to ³²
⁸⁰National Research Centre Kurchatov Institute, Moscow, Russia, associated to ⁴¹
⁸¹National Research University Higher School of Economics, Moscow, Russia, associated to ⁴²
⁸²National University of Science and Technology "MISIS", Moscow, Russia, associated to ⁴¹
⁸³National Research Tomsk Polytechnic University, Tomsk, Russia, associated to ⁴¹
⁸⁴DS4DS, La Salle, Universitat Ramon Llull, Barcelona, Spain, associated to ⁴⁵
⁸⁵University of Michigan, Ann Arbor, United States, associated to ⁶⁸
^aUniversidade Federal do Triângulo Mineiro (UFTM), Uberaba-MG, Brazil
^bHangzhou Institute for Advanced Study, UCAS, Hangzhou, China
^cUniversità di Bari, Bari, Italy
^dUniversità di Bologna, Bologna, Italy
^eUniversità di Cagliari, Cagliari, Italy
^fUniversità di Ferrara, Ferrara, Italy
^gUniversità di Firenze, Firenze, Italy
^hUniversità di Genova, Genova, Italy
ⁱUniversità degli Studi di Milano, Milano, Italy
^jUniversità di Milano Bicocca, Milano, Italy
^kUniversità di Modena e Reggio Emilia, Modena, Italy
^lUniversità di Padova, Padova, Italy
^mScuola Normale Superiore, Pisa, Italy
ⁿUniversità di Pisa, Pisa, Italy
^oUniversità della Basilicata, Potenza, Italy
^pUniversità di Roma Tor Vergata, Roma, Italy
^qUniversità di Siena, Siena, Italy
^rUniversità di Urbino, Urbino, Italy
^sMSU - Iligan Institute of Technology (MSU-IIT), Iligan, Philippines
^tAGH - University of Science and Technology, Faculty of Computer Science, Electronics and Telecommunications, Kraków, Poland
^uP.N. Lebedev Physical Institute, Russian Academy of Science (LPI RAS), Moscow, Russia
^vNovosibirsk State University, Novosibirsk, Russia
^wDepartment of Physics and Astronomy, Uppsala University, Uppsala, Sweden
^xHanoi University of Science, Hanoi, Vietnam

Abstract: The first search for the doubly heavy Ω_{bc}^0 baryon and a search for the Ξ_{bc}^0 baryon are performed using pp collision data collected via the LHCb experiment from 2016 to 2018 at a centre-of-mass energy of 13 TeV, corresponding to an integrated luminosity of 5.2 fb^{-1} . The baryons are reconstructed via their decays to $\Lambda_c^+\pi^-$ and $\Xi_c^+\pi^-$. No significant excess is found for invariant masses between 6700 and 7300 MeV/c^2 , in a rapidity range from 2.0 to 4.5 and a transverse momentum range from 2 to 20 MeV/c . Upper limits are set on the ratio of the Ω_{bc}^0 and Ξ_{bc}^0 production cross-section times the branching fraction to $\Lambda_c^+\pi^-$ ($\Xi_c^+\pi^-$) relative to that of the Λ_b^0 (Ξ_b^0) baryon, for different lifetime hypotheses, at 95% confidence level. The upper limits range from 0.5×10^{-4} to 2.5×10^{-4} for the $\Omega_{bc}^0 \rightarrow \Lambda_c^+\pi^-$ ($\Xi_{bc}^0 \rightarrow \Lambda_c^+\pi^-$) decay, and from 1.4×10^{-3} to 6.9×10^{-3} for the $\Omega_{bc}^0 \rightarrow \Xi_c^+\pi^-$ ($\Xi_{bc}^0 \rightarrow \Xi_c^+\pi^-$) decay, de-

pending on the considered mass and lifetime of the Ω_{bc}^0 (Ξ_{bc}^0) baryon.

Keywords: B physics, quarkonium, spectroscopy, heavy quark production

DOI: 10.1088/1674-1137/ac0c70

I. INTRODUCTION

The constituent quark model was initially proposed by Murray Gell-Mann [1] and George Zweig [2] for classification of hadrons formed from light quarks (u , d , s) and understanding their quantum numbers. It was later extended to hadrons containing heavy c or b quarks [3]. In addition to baryons containing a single heavy quark, the theory also predicts baryons comprising two heavy quarks. Such doubly heavy baryons provide a unique probe for quantum chromodynamics, the gauge theory of strong interactions. In 2017, the LHCb collaboration reported the first observation of the Ξ_{cc}^{++} baryon containing two charm quarks through the decay $\Xi_{cc}^{++} \rightarrow \Lambda_c^+ K^- \pi^+ \pi^+$ [4].¹⁾ The Ξ_{cc}^{++} state was later confirmed in the decay to $\Xi_c^+ \pi^+$ [5]. Its lifetime, mass and production cross-section were subsequently measured [6-8]. To date, no baryons containing one b and one c quark, or two b quarks, have been observed experimentally. An observation would enrich our knowledge of baryon spectroscopy and improve our understanding of the quark structure inside baryons.

The ground-state baryons containing one b and one c quark, the Ω_{bc}^0 (bcs), Ξ_{bc}^0 (bcd) and Ξ_{bc}^+ (bcu) states, have been considered within various theoretical models. Most studies predict the masses of the Ω_{bc}^0 and Ξ_{bc}^0 baryons to be between 6700 and 7200 MeV/ c^2 [9-25].

The lifetime of the Ω_{bc}^0 baryon is predicted to be 0.22 ± 0.04 ps [14], while the lifetime of Ξ_{bc}^0 is predicted to be in the range of 0.09 to 0.28 ps [14, 23, 26, 27]. The production cross-section of the Ξ_{bc}^0 baryon in proton-proton (pp) collisions at a centre-of-mass energy $\sqrt{s} = 14$ TeV is expected to lie in the range between 19 to 39 nb, derived from Ref. [28], in the Ξ_{bc}^0 pseudorapidity (η)

range of $1.9 < \eta < 4.9$, depending on the required minimum value of the momentum component transverse to the beam direction (p_T) of the Ξ_{bc}^0 particle. Recently, the LHCb experiment found no significant Ξ_{bc}^0 baryon signal in the predicted mass range using the $\Xi_{bc}^0 \rightarrow D^0 p K^-$ decay mode [29].

This article reports the first search for the Ω_{bc}^0 baryon and a new search for the Ξ_{bc}^0 baryon, both via decay chains $\Lambda_c^+ \pi^-$ with $\Lambda_c^+ \rightarrow p K^- \pi^+$ or $\Xi_c^+ \pi^-$ with $\Xi_c^+ \rightarrow p K^- \pi^+$ in the LHCb experiment. Examples of Feynman diagrams of the four signal decay modes are shown in Fig. 1. There are few theoretical predictions on the branching fractions of these decay modes. Ref. [30] predicts the branching fractions of the $\Omega_{bc}^0 \rightarrow \Xi_c^+ \pi^-$ and $\Xi_{bc}^0 \rightarrow \Lambda_c^+ \pi^-$ decays to be 1.6×10^{-7} and 3.0×10^{-7} , respectively. However, uncertainties are not quoted. Inputs from experimental studies are necessary to deepen our understanding of the properties of Ω_{bc}^0 and Ξ_{bc}^0 baryons, and can provide valuable reference for future searches. Besides, the distinct experimental signatures of these decays make it promising to search for them in the LHCb experiment considering the high detection efficiency of the LHCb detector.

The Ω_{bc}^0 and Ξ_{bc}^0 baryons are not differentiated and are collectively denoted as H_{bc}^0 hereafter, unless otherwise stated. The production cross-section times branching fraction of $H_{bc}^0 \rightarrow \Lambda_c^+ \pi^-$ ($H_{bc}^0 \rightarrow \Xi_c^+ \pi^-$) decay is measured relative to that of the control channel $\Lambda_b^0 \rightarrow \Lambda_c^+ \pi^-$ ($\Xi_b^0 \rightarrow \Xi_c^+ \pi^-$). This takes advantage of identical final-state particles and similar topology. The search is performed in the mass range between 6700 and 7300 MeV/ c^2 using the pp collision data collected with

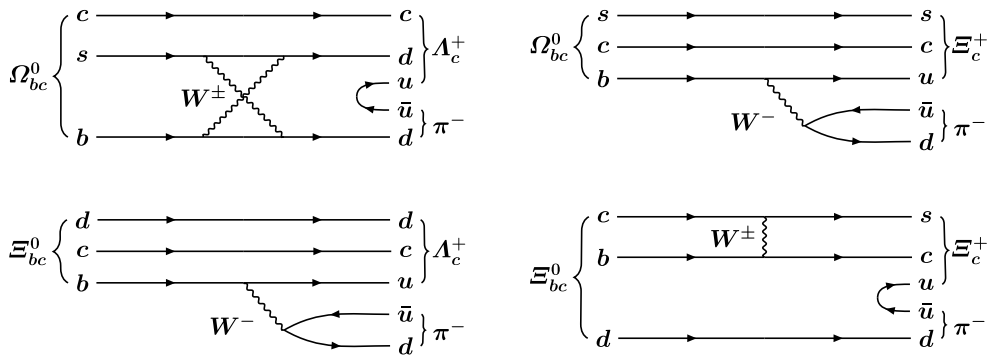


Fig. 1. Examples of Feynman diagrams for the $\Omega_{bc}^0 \rightarrow \Lambda_c^+ \pi^-$, $\Omega_{bc}^0 \rightarrow \Xi_c^+ \pi^-$, $\Xi_{bc}^0 \rightarrow \Lambda_c^+ \pi^-$ and $\Xi_{bc}^0 \rightarrow \Xi_c^+ \pi^-$ decays.

1) The inclusion of charge-conjugate modes is implied throughout this paper.

the LHCb experiment at $\sqrt{s} = 13$ TeV, corresponding to an integrated luminosity of 5.2 fb^{-1} . The H_{bc}^0 baryons are reconstructed in the fiducial region of rapidity (y) between 2.0 and 4.5 and with p_T between 2 and 20 MeV/ c .

II. DETECTOR AND SIMULATION

The LHCb detector [31, 32] is a single-arm forward spectrometer covering the pseudorapidity range $2 < \eta < 5$, designed for the study of particles containing b or c quarks. The detector includes a high-precision tracking system consisting of a silicon-strip vertex detector surrounding the pp interaction region [33], a large-area silicon-strip detector located upstream of a dipole magnet with a bending power of approximately 4 Tm, and three stations of silicon-strip detectors and straw drift tubes [34] placed downstream of the magnet. The tracking system provides a measurement of the momentum, p , of charged particles with a relative uncertainty that varies from 0.5% at low momentum to 1.0% at 200 MeV/ c . The minimum distance of a track to a primary pp collision vertex (PV), the impact parameter (IP), is measured with a resolution of $(15 + 29/p_T) \mu\text{m}$, where p_T is in MeV/ c . Different types of charged hadrons are distinguished using information from two ring-imaging Cherenkov detectors [35]. Photons, electrons, and hadrons are identified by a calorimeter system consisting of scintillating-pad and preshower detectors, and an electromagnetic and a hadronic calorimeter. Muons are identified by a system composed of alternating layers of iron and multiwire proportional chambers [36]. The online event selection is performed by a trigger [37], which consists of a hardware stage, based on information from the calorimeter and muon systems, followed by a software stage, which applies a full event reconstruction. At the hardware trigger stage, events are required to have at least one hadron with E_T larger than 3.5 GeV. The software trigger requires a two-, three-, or four-track secondary vertex with a significant displacement from any PV. At least one charged particle must have $p_T > 1.6$ MeV/ c and be inconsistent with originating from any PV. A multivariate algorithm [38, 39] is used for the identification of secondary vertices consistent with the decay of a b hadron.

Simulated samples are produced to model the effects of the detector acceptance and the imposed selection requirements. In the simulation, pp collisions are generated using PYTHIA [40, 41] with a specific LHCb configuration [42]. A dedicated generator, GENXICC2.0, is used to simulate the H_{bc}^0 baryon production [43], with the mass and lifetime of the H_{bc}^0 baryon set to $m(H_{bc}^0) = 6900$ MeV/ c^2 and $\tau(H_{bc}^0) = 0.4$ ps. Simulation samples with different mass (6700–7300 MeV/ c^2) and lifetime (0.2–0.4 ps) hypotheses are obtained using a weighting technique with the generator level information on signal.

Decays of unstable particles are described by EVTGEN [44], in which final-state radiation is generated using PHOTOS [45]. The interaction of the generated particles with the detector, and its response, is implemented using the GEANT4 toolkit [46, 47] as described in Ref. [48]. For the two control channels, $\Lambda_b^0 \rightarrow \Lambda_c^+\pi^-$ and $\Xi_b^0 \rightarrow \Xi_c^+\pi^-$, PYTHIA is used to simulate the pp collisions and the production of the Λ_b^0 and Ξ_b^0 baryons.

III. RECONSTRUCTION AND SELECTION

For both the H_{bc}^0 signal and the control channels, the $\Lambda_c^+, \Xi_c^+ \rightarrow pK^-\pi^+$ candidates are reconstructed from three charged particles identified as a proton, kaon and pion, respectively. The tracks are required to have good quality, and to be inconsistent with originating from any PV in the event. The tracks must also form a common vertex of good fit quality. The Λ_c^+ (Ξ_c^+) candidate is required to have an invariant mass in the range 2271–2301 MeV/ c^2 (2450–2488 MeV/ c^2), corresponding to approximately six times the Λ_c^+ (Ξ_c^+) mass resolution, and to be inconsistent with originating from any PV. In the sample of selected Λ_c^+ (Ξ_c^+) candidates, there is a sizable background contamination from decays of other particles, such as D^+ (D_s^+) decays to $K^-\pi^+\pi^+$ ($K^-K^+\pi^+$) with a charged pion (kaon) misidentified as a proton, and background from $\phi\pi^+$ combinations where in $\phi \rightarrow K^-K^+$ decays a kaon is misidentified as a proton. Such background candidates are rejected if the $K^-\pi^+\pi^+$, $K^-K^+\pi^+$ or K^-K^+ invariant mass is consistent with the known D^+ , D_s^+ or ϕ mass [49], respectively, when a charged pion (kaon) hypothesis is assigned to the proton candidate.

An additional charged particle identified as a pion and, with p_T greater than 0.2 MeV/ c , is combined with the Λ_c^+ (Ξ_c^+) candidate to form an H_{bc}^0 candidate. The H_{bc}^0 candidates must have a vertex with good fit quality, a decay time larger than 0.05 ps, a p_T greater than 2 MeV/ c and a scalar sum of the p_T of the final-state particles greater than 5 MeV/ c . Furthermore, the H_{bc}^0 candidates are required to be consistent with originating from a PV. To avoid contributions from duplicate tracks, the selected candidates are rejected if the angle between any pair of the final-state particle tracks with same charge is smaller than 0.5 mrad.

A boosted decision tree (BDT) classifier [50, 51] implemented in the TMVA toolkit [52, 53] is used to further suppress combinatorial background. A simulated signal sample in the mass range 6846–6954 MeV/ c^2 and a background sample formed by candidates in an upper mass sideband region (7500–9000 MeV/ c^2) are used to train the BDT classifier. Four different categories of variable are used as the BDT input. The first category exploits the non-zero lifetime of H_{bc}^0 baryons and a displacement of their vertices from any PV in the event. The

variables comprise the χ_{IP}^2 of all final-state particles forming the Λ_c^+ (Ξ_c^+) and H_{bc}^0 candidates with respect to their associated PV, where χ_{IP}^2 is defined as the difference in the vertex-fit χ^2 of a given PV reconstructed with and without the particle under consideration, and the associated PV is the one with respect to which the H_{bc}^0 candidate has the smallest χ_{IP}^2 ; the sum of χ_{IP}^2 of the four final-state particles; and χ^2 of the flight distance of the Λ_c^+ (Ξ_c^+) and H_{bc}^0 candidates. The second category consists of kinematic variables, including p_{T} of the final-state particles and the Λ_c^+ (Ξ_c^+) and H_{bc}^0 candidates, and the angle between the H_{bc}^0 momentum vector and the displacement vector pointing from the associated PV to the H_{bc}^0 decay vertex. The third category comprises the vertex-fit χ^2 of the Λ_c^+ (Ξ_c^+) and H_{bc}^0 candidates, and χ^2 of a kinematic fit [54] of the signal decay chain constraining the H_{bc}^0 candidate to originate from the associated PV. The fourth category consists of identification variables of the final-state particles.

The BDT threshold is chosen to maximize the figure of merit, $\varepsilon/(\frac{\alpha}{2} + \sqrt{B})$ [55]. Here, ε is the selection efficiency of signal candidates determined from simulation, B is the expected background number in the signal mass region, and $\alpha = 5$ is the signal significance. This threshold is estimated using the signal sample simulated

with the default mass and lifetime values. The same selection is applied to the control modes.

IV. YIELD DETERMINATION

To improve the resolution of the mass of the H_{bc}^0 candidates, the $\Lambda_c^+\pi^-$ ($\Xi_c^+\pi^-$) invariant mass is calculated after constraining the Λ_c^+ (Ξ_c^+) mass to its known value [49] and requiring the H_{bc}^0 candidate to be consistent with originating from its associated PV. The obtained invariant mass distributions of H_{bc}^0 candidates, $m(\Lambda_c^+\pi^-)$ and $m(\Xi_c^+\pi^-)$, are shown in Fig. 2. To search for the H_{bc}^0 signals, the mass distributions are fitted using an unbinned maximum-likelihood fit. A double-sided Crystal Ball function [56] is used to model the signal, with tail parameters fixed from simulation, and the peak position and width allowed to vary in the fit. The background shape is interpolated from a double-exponential fit to a lower (6100–6650 MeV/ c^2) and an upper (7500–9000 MeV/ c^2) sideband region of the $\Lambda_c^+\pi^-$ ($\Xi_c^+\pi^-$) mass distribution. No significant excess is observed across the searched mass range.

The $\Lambda_c^+\pi^-$ and $\Xi_c^+\pi^-$ invariant mass distributions of the selected $\Lambda_b^0 \rightarrow \Lambda_c^+(\rightarrow pK^-\pi^+)\pi^-$ and $\Xi_b^0 \rightarrow \Xi_c^+(\rightarrow pK^-\pi^+)\pi^-$ candidates are shown in Fig. 3. The yields are obtained from unbinned maximum-likelihood fits to the

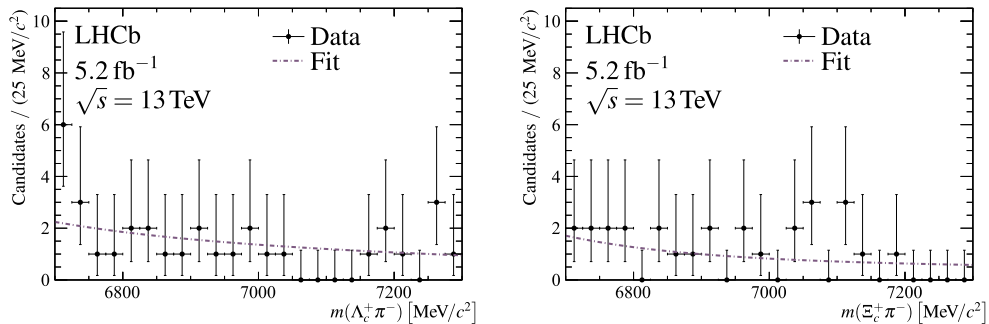


Fig. 2. (color online) Invariant mass distributions of selected (left) $H_{bc}^0 \rightarrow \Lambda_c^+\pi^-$ and (right) $H_{bc}^0 \rightarrow \Xi_c^+\pi^-$ candidates (black points), together with results of the background only fit (brown dashed line).

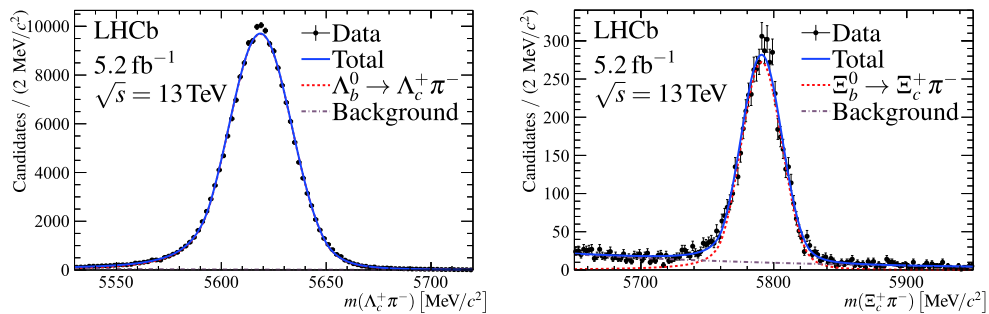


Fig. 3. (color online) Invariant mass distributions of (left) $\Lambda_b^0 \rightarrow \Lambda_c^+(\rightarrow pK^-\pi^+)\pi^-$ and (right) $\Xi_b^0 \rightarrow \Xi_c^+(\rightarrow pK^-\pi^+)\pi^-$ candidates with the fit results overlaid (blue solid line). The black points represent the data, the red dashed line represents the signal contribution, and the gray dashed line represents the combinatorial background.

invariant mass distributions, using the fit model described above. The yields are determined to be $191\,000 \pm 500$ and 5490 ± 80 for $\Lambda_b^0 \rightarrow \Lambda_c^+(\rightarrow pK^-\pi^+)\pi^-$ and $\Xi_b^0 \rightarrow \Xi_c^+(\rightarrow pK^-\pi^+)\pi^-$, respectively.

V. RATIO OF PRODUCTION CROSS-SECTIONS

The ratio \mathcal{R} of the H_{bc}^0 baryon production cross-section multiplied by the branching fraction of the $H_{bc}^0 \rightarrow \Lambda_c^+\pi^-$ ($H_{bc}^0 \rightarrow \Xi_c^+\pi^-$) decay relative to that of the Λ_b^0 (Ξ_b^0) baryon can be written as

$$\begin{aligned} \mathcal{R}(\Lambda_c^+\pi^-) &\equiv \frac{\sigma(pp \rightarrow H_{bc}^0 X) \mathcal{B}(H_{bc}^0 \rightarrow \Lambda_c^+(\rightarrow pK^-\pi^+)\pi^-)}{\sigma(pp \rightarrow \Lambda_b^0 X) \mathcal{B}(\Lambda_b^0 \rightarrow \Lambda_c^+(\rightarrow pK^-\pi^+)\pi^-)} \\ &= \frac{N(H_{bc}^0 \rightarrow \Lambda_c^+\pi^-)}{N(\Lambda_b^0 \rightarrow \Lambda_c^+\pi^-)} \cdot \frac{\varepsilon(\Lambda_b^0)}{\varepsilon(H_{bc}^0)}, \end{aligned} \quad (1)$$

$$\begin{aligned} \mathcal{R}(\Xi_c^+\pi^-) &\equiv \frac{\sigma(pp \rightarrow H_{bc}^0 X) \mathcal{B}(H_{bc}^0 \rightarrow \Xi_c^+(\rightarrow pK^-\pi^+)\pi^-)}{\sigma(pp \rightarrow \Xi_b^0 X) \mathcal{B}(\Xi_b^0 \rightarrow \Xi_c^+(\rightarrow pK^-\pi^+)\pi^-)} \\ &= \frac{N(H_{bc}^0 \rightarrow \Xi_c^+\pi^-)}{N(\Xi_b^0 \rightarrow \Xi_c^+\pi^-)} \cdot \frac{\varepsilon(\Xi_b^0)}{\varepsilon(H_{bc}^0)}, \end{aligned} \quad (2)$$

where N and ε are the signal yield and the efficiency for the corresponding decay modes, respectively. The efficiency accounts for the geometrical acceptance, trigger, reconstruction, and event selection. The \mathcal{R} is determined in the fiducial region $2 < y < 4.5$ and $2 < p_T < 20$ MeV/ c .

Efficiencies are determined from the simulated samples. The p_T distributions of Λ_b^0 and Ξ_b^0 baryons are not well modeled in simulation. To improve the description, a gradient boosted weighting method [57] is used to apply a kinematic correction on the p_T distributions of the Λ_b^0 and Ξ_b^0 decay products of the simulated control samples. With this correction, a good agreement on the Λ_b^0 and Ξ_b^0 p_T distribution is seen between the data and simulation. The track detection and particle identification efficiencies are calibrated with the data [58-60]. The imperfect modeling of input variables used in the BDT training can bias the efficiency estimation. To suppress such effects, ratios between the BDT response distribution of the background-subtracted data sample and that of the simulated sample are calculated using the control channel. The background subtraction is performed using the *sPlot* method [61] with $m(\Lambda_c^+\pi^-)$ and $m(\Xi_c^+\pi^-)$ as discriminating variables. These ratios are applied as correction weights to the simulated samples for all reconstructed decay modes.

The total efficiency ratio $\varepsilon(\Lambda_b^0)/\varepsilon(H_{bc}^0)$ is determined to be 3.18 ± 0.05 , and $\varepsilon(\Xi_b^0)/\varepsilon(H_{bc}^0)$ is calculated to be 3.00 ± 0.02 for $m(H_{bc}^0) = 6900$ MeV/ c^2 and $\tau(H_{bc}^0) = 0.4$ ps. The efficiency is larger for the control mode, mainly due to the longer lifetime of the Λ_b^0 and Ξ_b^0 baryons. The efficiency depends on the mass and lifetime hypotheses of the H_{bc}^0 state, and is evaluated from simulation. The kinematic properties of the fully simulated samples are weighted to match those of the generator-level sample to calculate the efficiency for different H_{bc}^0 mass and lifetime assumptions.

VI. SYSTEMATIC UNCERTAINTIES

Various sources of systematic uncertainties on \mathcal{R} are estimated and combined in quadrature. The effect of imperfect description of the mass distributions on the yield estimates is studied using alternative signal and background models. For the signal model, the Hypatia [62] function is used instead of the nominal double-sided Crystal Ball function. For the background model of the control modes, the nominal double-exponential function is replaced by a first-order polynomial function. As the background model for the H_{bc}^0 decay modes is interpolated from the sidebands, its uncertainty is evaluated by both replacing the nominal function with an exponential function and varying the sideband regions. The largest deviation with respect to the nominal result is taken as the corresponding uncertainty. In total, the associated systematic uncertainty is estimated to be 0.1% and 0.9% for $H_{bc}^0 \rightarrow \Lambda_c^+\pi^-$ and $H_{bc}^0 \rightarrow \Xi_c^+\pi^-$ decays, respectively.

In the \mathcal{R} ratios, systematic uncertainties arising from the track detection efficiency largely cancel, and the uncertainty due to limited size of simulation samples is determined to be 1.6% (0.7%) on $\mathcal{R}(\Lambda_c^+\pi^-)$ ($\mathcal{R}(\Xi_c^+\pi^-)$). The particle identification efficiency is determined in bins of particle momentum, pseudorapidity, and track multiplicity using control channels in the data [60]. As the particle identification variables have large dependencies on the momentum of the final-state particles, there are sizeable differences in these efficiencies between the control and signal channels, which do not cancel in the ratio measurement. Systematic effects arising from the choice of binning scheme are evaluated by varying the bin sizes and reevaluating the efficiency. The largest deviations from the nominal result, 1.7% and 2.1%, are assigned as the systematic uncertainty for the $H_{bc}^0 \rightarrow \Lambda_c^+\pi^-$ and $H_{bc}^0 \rightarrow \Xi_c^+\pi^-$ decays, respectively.

The Λ_c^+ (Ξ_c^+) mass resolution shows a difference between data and simulation, which affects the selection efficiency. It results in a 0.2% systematic uncertainty contribution for the $H_{bc}^0 \rightarrow \Xi_c^+\pi^-$ decay, while the contribution for the $H_{bc}^0 \rightarrow \Lambda_c^+\pi^-$ decay is below 0.1%. This systematic uncertainty is negligible compared to other sources.

The imperfect simulation of the signal and control modes are considered by applying corrections to the BDT response and kinematic properties of the simulated control mode samples. To assess the systematic uncertainty in these corrections, the correcting weights are varied within their uncertainties. The largest deviation from the nominal result is taken as the systematic uncertainty. Combining the uncertainties from the BDT response correction and the kinematic modeling of the simulated control samples gives an uncertainty of 1.6% for the $H_{bc}^0 \rightarrow \Lambda_c^+ \pi^-$ channel, and 3.0% for the $H_{bc}^0 \rightarrow \Xi_c^+ \pi^-$ channel. The analysis relies on the Ξ_{bc}^0 p_T model implemented in simulation. No systematic uncertainty is assigned to this model.

The algorithm used to compute the χ_{IP}^2 was updated during data collection, which causes a mismatch between data and simulation and introduces systematic effects in the efficiency estimation. The corresponding uncertainty was found to be 5% in the previous Ξ_{bc}^0 search [29]. Checks by varying the χ_{IP}^2 -related requirements show that the uncertainty well covers the change of result. Therefore, a 5% systematic uncertainty is assigned.

Table 1. Sources of systematic uncertainty obtained for an H_{bc}^0 mass of 6900 MeV/ c^2 and lifetime of 0.4 ps. The total is the quadratic sum of the individual systematic uncertainties.

	$H_{bc}^0 \rightarrow \Lambda_c^+ \pi^-$	$H_{bc}^0 \rightarrow \Xi_c^+ \pi^-$
Fit model	0.1%	0.9%
Size of simulated samples	1.6%	0.7%
Particle identification efficiency	1.7%	2.1%
Mass resolution	<0.1%	0.2%
Simulation model	1.6%	3.0%
χ_{IP}^2 simulation	5.0%	5.0%
Total	5.7%	6.3%

The systematic uncertainties are summarized in Table 1. The total systematic uncertainty is 5.7% for $H_{bc}^0 \rightarrow \Lambda_c^+ \pi^-$ and 6.3% for $H_{bc}^0 \rightarrow \Xi_c^+ \pi^-$, for a H_{bc}^0 mass of 6900 MeV/ c^2 and lifetime of 0.4 ps. These values of systematic uncertainties are also used for other assumed lifetime and mass hypotheses.

VII. RESULTS

No evidence for a Ω_{bc}^0 or a Ξ_{bc}^0 baryon is observed in the inspected mass range. Upper limits are set at 95% confidence level on the ratios $\mathcal{R}(\Lambda_c^+ \pi^-)$ and $\mathcal{R}(\Xi_c^+ \pi^-)$ under different mass and lifetime hypotheses for the Ω_{bc}^0 and Ξ_{bc}^0 baryons, using the asymptotic CL_s method implemented in the ROOSTATS framework [63, 64] considering the systematic uncertainties. The assumed masses of the Ω_{bc}^0 and Ξ_{bc}^0 baryons are varied from 6700 to 7300 MeV/ c^2 with a step size of 4 MeV/ c^2 , and the lifetime values of 0.2 ps, 0.3 ps, and 0.4 ps are considered. The calculated upper limits are shown in Fig. 4, as a function of the H_{bc}^0 mass. These results are obtained for the sum of the Ω_{bc}^0 and Ξ_{bc}^0 production and as such hold for the two individually.

VIII. CONCLUSIONS

The first search for the doubly heavy baryon Ω_{bc}^0 and a new search for the Ξ_{bc}^0 baryon in the mass range from 6700 to 7300 MeV/ c^2 are presented, using pp collision data collected at a centre-of-mass energy $\sqrt{s} = 13$ TeV with the LHCb experiment. The data set corresponds to an integrated luminosity of 5.2 fb $^{-1}$. The Ω_{bc}^0 (Ξ_{bc}^0) baryon is reconstructed in the $\Lambda_c^+ \pi^-$ and $\Xi_c^+ \pi^-$ decay modes. No evidence of a signal is found. Upper limits at 95% confidence level on the ratio of the Ω_{bc}^0 (Ξ_{bc}^0) production cross-section times its branching fraction relative to that of the Λ_b^0 (Ξ_b^0) baryon are calculated in the rapidity range

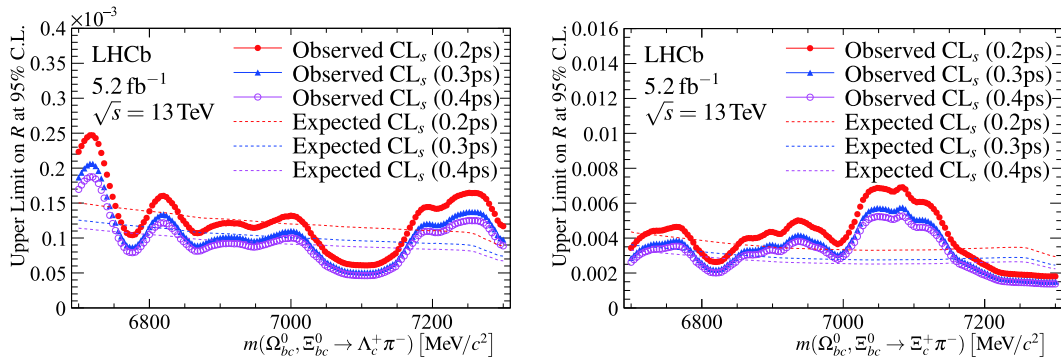


Fig. 4. (color online) Upper limits (dotted lines) on the ratio of production cross-section for Ω_{bc}^0 and Ξ_{bc}^0 via decays to (left) $\Lambda_c^+ \pi^-$ and (right) $\Xi_c^+ \pi^-$ to that of control channels $\Lambda_b^0 \rightarrow \Lambda_c^+ \pi^-$ and $\Xi_b^0 \rightarrow \Xi_c^+ \pi^-$. The dotted (dashed) colored lines represent the observed (expected) upper limits. The assumed lifetime hypotheses for the Ω_{bc}^0 (Ξ_{bc}^0) are 0.2 ps (red filled circles), 0.3 ps (blue triangles), and 0.4 ps (magenta open circles).

$2.0 < y < 4.5$ and transverse momentum range $2 < p_T < 20$ MeV/c under different Ω_{bc}^0 (Ξ_{bc}^0) mass and lifetime hypotheses. The upper limits range from 0.5×10^{-4} to 2.5×10^{-4} for the $\Omega_{bc}^0 \rightarrow \Lambda_c^+\pi^-$ ($\Xi_{bc}^0 \rightarrow \Lambda_c^+\pi^-$) decay, and from 1.4×10^{-3} to 6.9×10^{-3} for the $\Omega_{bc}^0 \rightarrow \Xi_c^+\pi^-$ ($\Xi_{bc}^0 \rightarrow \Xi_c^+\pi^-$) decay, for the considered lifetime and mass hypotheses. These results constitute the first limit on the production of the Ω_{bc}^0 baryon. Further

measurements will be possible with the larger data samples expected at the upgraded LHCb experiments [65] and with additional decay modes.

ACKNOWLEDGEMENTS

We express our gratitude to our colleagues in the CERN accelerator departments for the excellent performance of the LHC.

References

- [1] M. Gell-Mann, *Phys. Lett.* **8**, 214 (1964)
- [2] G. Zweig, in *An SU(3) model for strong interaction symmetry and its breaking. Version 2*, D. B. Lichtenberg and S. P. Rosen, eds., pp. 22-101, 1964
- [3] S. Fleck, B. Silvestre-Brac, and J. M. Richard, *Phys. Rev. D* **38**, 1519 (1988)
- [4] R. Aaij *et al.* (LHCb Collaboration), *Phys. Rev. Lett.* **119**, 112001 (2017), arXiv:1707.01621
- [5] R. Aaij *et al.* (LHCb Collaboration), *Phys. Rev. Lett.* **121**, 162002 (2018), arXiv:1807.01919
- [6] R. Aaij *et al.* (LHCb Collaboration), *Phys. Rev. Lett.* **121**, 052002 (2018), arXiv:1806.02744
- [7] R. Aaij *et al.* (LHCb Collaboration), *Chin. Phys. C* **44**, 022001 (2020), arXiv:1910.11316
- [8] R. Aaij *et al.* (LHCb Collaboration), *JHEP* **02**, 049 (2020), arXiv:1911.08594
- [9] E. Bagan, M. Chabab, and S. Narison, *Phys. Lett. B* **306**, 350 (1993)
- [10] R. Roncaglia, D. B. Lichtenberg, and E. Predazzi, *Phys. Rev. D* **52**, 1722 (1995), arXiv:hep-ph/9502251
- [11] D. B. Lichtenberg, R. Roncaglia, and E. Predazzi, *Phys. Rev. D* **53**, 6678 (1996), arXiv:hep-ph/9511461
- [12] D. Ebert *et al.*, *Z. Phys. C* **76**, 111 (1997), arXiv:hep-ph/9607314
- [13] B. Silvestre-Brac, *Prog. Part. Nucl. Phys.* **36**, 263 (1996)
- [14] V. V. Kiselev and A. K., *Phys. Usp.* **45**, 455 (2002), arXiv:hep-ph/0103169
- [15] K. Anikeev *et al.*, 2001, arXiv: hep-ph/0201071
- [16] D. Ebert, R. N. Faustov, V. O. Galkin *et al.*, *Phys. Rev. D* **66**, 014008 (2002), arXiv:hep-ph/0201217
- [17] D.-H. He *et al.*, *Phys. Rev. D* **70**, 094004 (2004), arXiv:hep-ph/0403301
- [18] C. Albertus, E. Hernandez, J. Nieves *et al.*, *Eur. Phys. J. A* **32**, 183 (2007), Erratum: *Eur. Phys. J. A* **36**, 119 (2008)
- [19] W. Roberts and M. Pervin, *Int. J. Mod. Phys. A* **23**, 2817 (2008), arXiv:0711.2492
- [20] J.-R. Zhang and M.-Q. Huang, *Phys. Rev. D* **78**, 094007 (2008), arXiv:0810.5396
- [21] S. M. Gerasyuta and E. E. Matskevich, *Int. J. Mod. Phys. E* **18**, 1785 (2009), arXiv:0803.3497
- [22] K. Azizi, T. M. Aliev, and M. Savci, *J. Phys. Conf. Ser.* **556**, 012016 (2014)
- [23] M. Karliner and J. L. Rosner, *Phys. Rev. D* **90**, 094007 (2014), arXiv:1408.5877
- [24] Z. Shah and A. K. Rai, *Eur. Phys. J. C* **77**, 129 (2017), arXiv:1702.02726
- [25] Z. S. Brown, W. Detmold, S. Meinel *et al.*, *Phys. Rev. D* **90**, 094507 (2014), arXiv:1409.0497
- [26] V. V. Kiselev, A. K. Likhoded, and A. I. Onishchenko, *Eur. Phys. J. C* **16**, 461 (2000), arXiv:hep-ph/9901224
- [27] H.-Y. Cheng and F. Xu, *Phys. Rev. D* **99**, 073006 (2019), arXiv:1903.08148
- [28] J.-W. Zhang *et al.*, *Phys. Rev. D* **83**, 034026 (2011), arXiv:1101.1130
- [29] R. Aaij *et al.* (LHCb Collaboration), *JHEP* **11**, 095 (2020), arXiv:2009.02481
- [30] W. Wang, F.-S. Yu, and Z.-X. Zhao, *Eur. Phys. J. C* **77**, 781 (2017), arXiv:1707.02834
- [31] A. A. Alves Jr. *et al.* (LHCb Collaboration), *JINST* **3**, S08005 (2008)
- [32] R. Aaij *et al.* (LHCb Collaboration), *Int. J. Mod. Phys. A* **30**, 1530022 (2015), arXiv:1412.6352
- [33] R. Aaij *et al.*, *JINST* **9**, P09007 (2014), arXiv:1405.7808
- [34] P. d'Argent *et al.*, *JINST* **12**, P11016 (2017), arXiv:1708.00819
- [35] M. Adinolfi *et al.*, *Eur. Phys. J. C* **73**, 2431 (2013), arXiv:1211.6759
- [36] A. A. Alves Jr. *et al.*, *JINST* **8**, P02022 (2013), arXiv:1211.1346
- [37] R. Aaij *et al.*, *JINST* **8**, P04022 (2013), arXiv:1211.3055
- [38] V. V. Gligorov and M. Williams, *JINST* **8**, P02013 (2013), arXiv:1210.6861
- [39] T. Likhomanenko *et al.*, *J. Phys. Conf. Ser.* **664**, 082025 (2015)
- [40] T. Sjöstrand, S. Mrenna, and P. Skands, *Comput. Phys. Commun.* **178**, 852 (2008), arXiv:0710.3820
- [41] T. Sjöstrand, S. Mrenna, and P. Skands, *JHEP* **05**, 026 (2006), arXiv:hep-ph/0603175
- [42] I. Belyaev *et al.*, *J. Phys. Conf. Ser.* **331**, 032047 (2011)
- [43] C.-H. Chang, J.-X. Wang, and X.-G. Wu, *Comput. Phys. Commun.* **181**, 1144 (2010), arXiv:0910.4462
- [44] D. J. Lange, *Nucl. Instrum. Meth. A* **462**, 152 (2001)
- [45] N. Davidson, T. Przedzinski, and Z. Was, *Comput. Phys. Commun.* **199**, 86 (2016), arXiv:1011.0937
- [46] J. Allison *et al.* (Geant4 Collaboration), *IEEE Trans. Nucl. Sci.* **53**, 270 (2006)
- [47] S. Agostinelli *et al.* (Geant4 Collaboration), *Nucl. Instrum. Meth. A* **506**, 250 (2003)
- [48] M. Clemencic *et al.*, *J. Phys. Conf. Ser.* **331**, 032023 (2011)
- [49] P. A. Zyla *et al.* (Particle Data Group), *Prog. Theor. Exp. Phys.* **2020**, 083C01 (2020)
- [50] L. Breiman, J. H. Friedman, R. A. Olshen *et al.*, Wadsworth international group, Belmont, California, USA, 1984
- [51] Y. Freund and R. E. Schapire, *J. Comput. Syst. Sci.* **55**, 119 (1997)
- [52] H. Voss, A. Hoecker, J. Stelzer *et al.*, *PoS ACAT*, 040 (2007)
- [53] A. Hocker *et al.*, arXiv: physics/0703039

- [54] W. D. Hulsbergen, Nucl. Instrum. Meth. A **552**, 566 (2005), arXiv:[physics/0503191](#)
- [55] G. Punzi, eConf **C030908**, MODT002 (2003), arXiv:[physics/0308063](#)
- [56] T. Skwarnicki, *A study of the radiative cascade transitions between the Upsilon-prime and Upsilon resonances*, PhD thesis, Institute of Nuclear Physics, Krakow, 1986, DESY-F31-86-02
- [57] A. Rogozhnikov, J. Phys. Conf. Ser. **762**, 012036 (2016), arXiv:1608.05806
- [58] R. Aaij *et al.* (LHCb Collaboration), *JINST* **10**, P02007 (2015), arXiv:[1408.1251](#)
- [59] L. Anderlini *et al.*, LHCb-PUB-2016-021, 2016
- [60] R. Aaij *et al.*, Eur. Phys. J. Tech. Instr. **6**, 1 (2018), arXiv:[1803.00824](#)
- [61] M. Pivk and F. R. Le Diberder, Nucl. Instrum. Meth. A **555**, 356 (2005), arXiv:[physics/0402083](#)
- [62] D. Martínez Santos and F. Dupertuis, Nucl. Instrum. Meth. A **764**, 150 (2014), arXiv:[1312.5000](#)
- [63] L. Moneta *et al.*, PoS **ACAT2010**, 057 (2010), arXiv:[1009.1003](#)
- [64] G. Cowan, K. Cranmer, E. Gross *et al.*, Eur. Phys. J. C **71**, 1554 (2011), arXiv:[1007.1727](#)
- [65] R. Aaij *et al.* (LHCb), arXiv:1808.08865